Neutrino-nucleus interactions and the short-range structure of nuclei

F. Cavanna[a], O. Palamara[a], R. Schiavilla[b,c], M. Soderberg[a,e], and R.B. Wiringa[d]

[a] *Fermi National Acclerator Laboratory, Batavia, IL 60510*

[b] *Thomas Jefferson National Accelerator Facility, Newport News, VA 23606*

[c] *Department of Physics, Old Dominion University, Norfolk, VA 23529*

[d] *Physics Division, Argonne National Laboratory, Argonne, IL 60439*

[e] *Department of Physics, Syracuse University, Syracuse, NY 13244*

(Dated: January 5, 2015)

I. INTRODUCTION

The atomic nucleus was discovered by Rutherford in 1911 [1], who also classified nuclear physics as the *unclear physics*. This characterization continues to apply to several areas of nuclear physics even today. The fundamental degrees of freedom in nuclei are believed to be quarks and gluons; however, due to color confinement, free quarks are not detectable. At low energies, quantum chromodynamics, which governs the behavior of interacting quarks and gluons, does not have simple solutions. The observed degrees of freedom of nuclear physics are hadrons, protons and neutrons in particular.

In the past century many interesting models were developed to explain the systematic trends in the low-energy properties of stable and near stable atomic nuclei. They include, for example, the liquid-drop model, the compound-nucleus model, the shell model, the optical model, the collective model, and the interacting boson model. These models have provided deep insights into nuclear structure and reactions, and have been quite successful in correlating many of the nuclear properties. Most of them can be related to the shell model which describes the general theory of quantum liquid drops.

All the nuclear models tacitly assume that nuclei are made up of interacting protons and neutrons, collectively referred to as nucleons. Within this approximation a general theory can be developed for all low-energy phenomena displayed by interacting nucleons, ranging from the deuteron to neutron stars. The simplest version of this theory describes low-energy nuclear systems as those composed of nucleons interacting via many-body potentials and many-body electroweak currents. We call it the "basic model." It is likely that the shell model and other models of nuclei can be considered as suitable approximations of this theory for various energy and mass regions of nuclear systems.

The basic model assumes that a Hamiltonian,

$$H = \sum_i \left(m_i + \frac{\mathbf{p}_i^2}{2\, m_i} \right) + \sum_{i<j} v_{ij} + \sum_{i<j<k} V_{ijk} + \ \dots \ , \tag{1.1}$$

provides a good approximation to the energy of interacting nucleons. The subscripts $i, j, k, \dots$ label the nucleons in the system. The mass m_i is that of a proton or neutron according to the nature of nucleon i. Much effort has been devoted over the past several decades on the development of nuclear potentials. Modern two-nucleon (NN) potentials v_{ij} consist of a long-range component induced by one-pion exchange and intermediate- to short-range

components which are modeled either phenomenologically, as in the Argonne v_{18} (AV18) potential [2], or by scalar and vector meson-exchanges, as in the CD-Bonn potential [3], or by a combination of two-pion-exchange mechanisms and contact two-nucleon terms, such as in chiral-effective-field-theory [4]. All these models fit the extensive NN database (pp and np cross sections and polarization observables) for energies up to the pion production threshold with a $\chi^2 \simeq 1$. However, it is by now an established fact that NN potentials alone fail to predict the spectra of light nuclei [5], cross sections and analyzing powers in Nd scattering at low [6] and intermediate [7] energies, and the nuclear matter equilibrium properties [8].

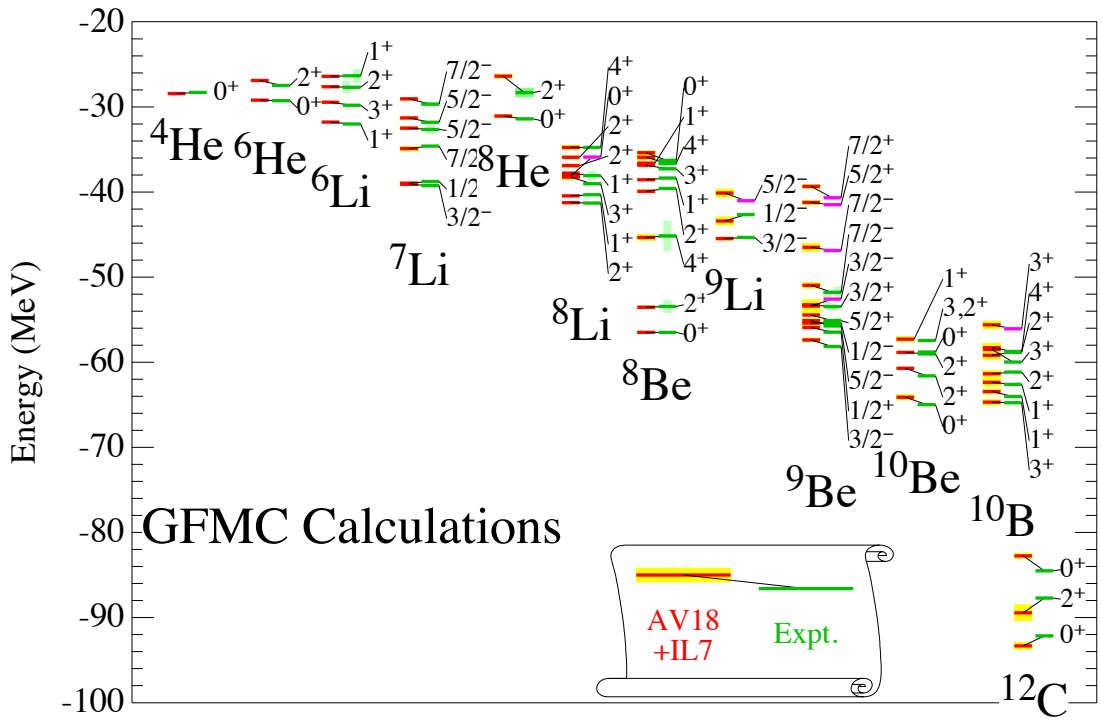

FIG. 1: The low-lying energy spectra of nuclei with mass number A=4–12, obtained in exact *ab initio* Green's function Monte Carlo (GFMC) calculations with the AV18/IL7 Hamiltonian.

Models of the three-nucleon potential include two- and three-pion exchange [9, 10] as well as short-range repulsive terms. In the Illinois model 7 (IL7), for which the most extensive

calculations have been carried out to date, these multi-pion exchange components involve excitation of intermediate Δ resonances. The IL7 strength is determined by four parameters which are fixed by a best fit to the energies of about 17 low-lying states of nuclei in the mass range $A \leq 10$, obtained in combination with the AV18 NN potential, in exact *ab initio* quantum Monte Carlo calculations. The resulting AV18/IL7 Hamiltonian then leads to predictions [11] of ~ 100 ground- and excited-state energies up to A=12, including the ^{12}C ground- and Hoyle-state energies, in good agreement with the corresponding empirical values. Some of these results are displayed in Fig. 1; in particular, for ^{12}C the predicted ground-state energy and root-mean-square charge radius are [12] –93.3(4) MeV and 2.46(2) fm, respectively, in excellent agreement with the empirical values of –92.16 MeV and 2.471(5) fm.

II. SHORT-RANGE STRUCTURE OF NUCLEI

The potential v_{ij} that binds protons and neutrons together in the atomic nucleus is characterized by a strong repulsion at short ($\lesssim 0.5$ fm) distances, and a strong coupling between spatial and spin and isospin degrees of freedom in pairs of nucleons at intermediate to large ($\gtrsim 1$ fm) separations. This "tensor" character, mostly due to single- and multi-pion exchanges, of v_{ij} binds the deuteron—the simplest nucleus consisting of a proton and neutron—and couples the S- and D-waves into a ground state with a large non-spherical component. This is in marked contrast to systems such as the hydrogen atom where the dominant $1/r$ Coulomb potential leads to a spherical ground state.

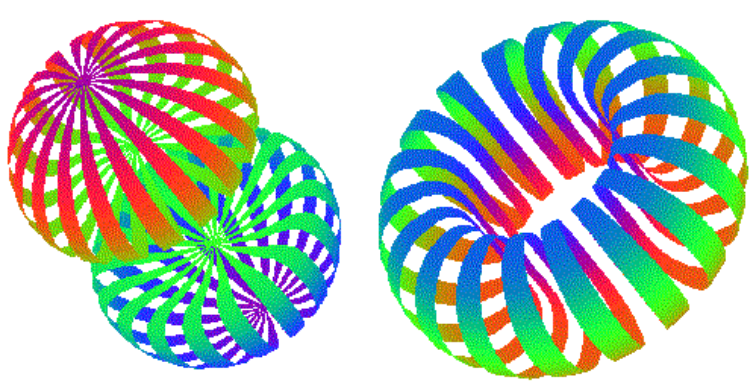

FIG. 2: Constant density surfaces for a polarized deuteron in the $M = \pm 1$ (left) and $M = 0$ (right) states.

While many systems share a trait of short-range repulsion, the tensor character is unique

to the nuclear force. In the deuteron, which has total angular momentum J=1 and can therefore be oriented in a specific direction, for example by an external electromagnetic field, with spin projections M=+1 (parallel), M=–1 (antiparallel), and M=0 (perpendicular), it leads to the unusual shapes in Fig. 2 [13]—the length of the dumbbell and the diameter of the torus are both about 1.5 fm. Their presence has been confirmed in electron scattering experiments on polarized deuterons.

The correlations induced by the central and tensor components of the potential v_{ij} affect many nuclear properties. In nuclei with mass number $A \geq 3$ the pair density distribution of a neutron and proton at separation $\mathbf{r}$ and with their spins coupled to $S = 1$ (a deuteron-like pair) depends strongly on the spin projections $M_S = \pm 1, 0$, i.e., on the relative orientation between $\mathbf{r}$ and the spin projection [13]. At a separation $r \simeq 1$ fm the difference in potential energy between the two configurations in which the neutron and proton are located either along the z-axis (the spin quantization axis) or in the xy plane is large and positive (+200 to +300 MeV) when $M_S = 0$, and large in magnitude but of opposite sign (–150 to –100 MeV) when $M_S = \pm 1$. As a consequence of the energy difference between these two extreme configurations, np pairs in $S = 1$ are mostly confined to the xy-plane for $M_S = 0$ and mostly along the z-axis for $M_S = \pm 1$, giving rise to the peculiar toroidal- and dumbbell-like equi-density surfaces already shown in Fig. 2 for the deuteron; the holes in the center of the torus and dumbbell are due to the short-range repulsion. It turns out [13] that these $S = 1$ np-pair densities in different nuclei can be scaled, through a single scaling factor R_{Ad}, to lie on universal surfaces for $r \lesssim 2$ fm—the dumbbell and torus of the deuteron.

Other nuclear properties strongly affected by correlations are the momentum distributions of nucleons and nucleon pairs in nuclei, which provide useful insights into various reactions on nuclei, such as $(e, e'p)$ and $(e, e'pp/np)$ electro-disintegration processes or neutrino-nucleus interaction experiments. Single-nucleon momentum distributions in s- and p-shell nuclei are displayed in Fig. 3 [14, 15]. Their shape shows a smooth progression as nucleons are added. As the mass number A increases, the nuclei become more tightly bound, and the fraction of nucleons at zero momentum decreases. As nucleons are added to the p-shell, the distribution at low momenta becomes broader, and develops a peak at finite momentum k. The sharp change in slope near $k = 2$ fm^{-1} to a broad shoulder is present in all these nuclei and is attributable to the strong tensor correlations induced by the pion-exchange part of the potential v_{ij}. Above $k = 4$ fm^{-1}, the bulk of the momentum density comes from

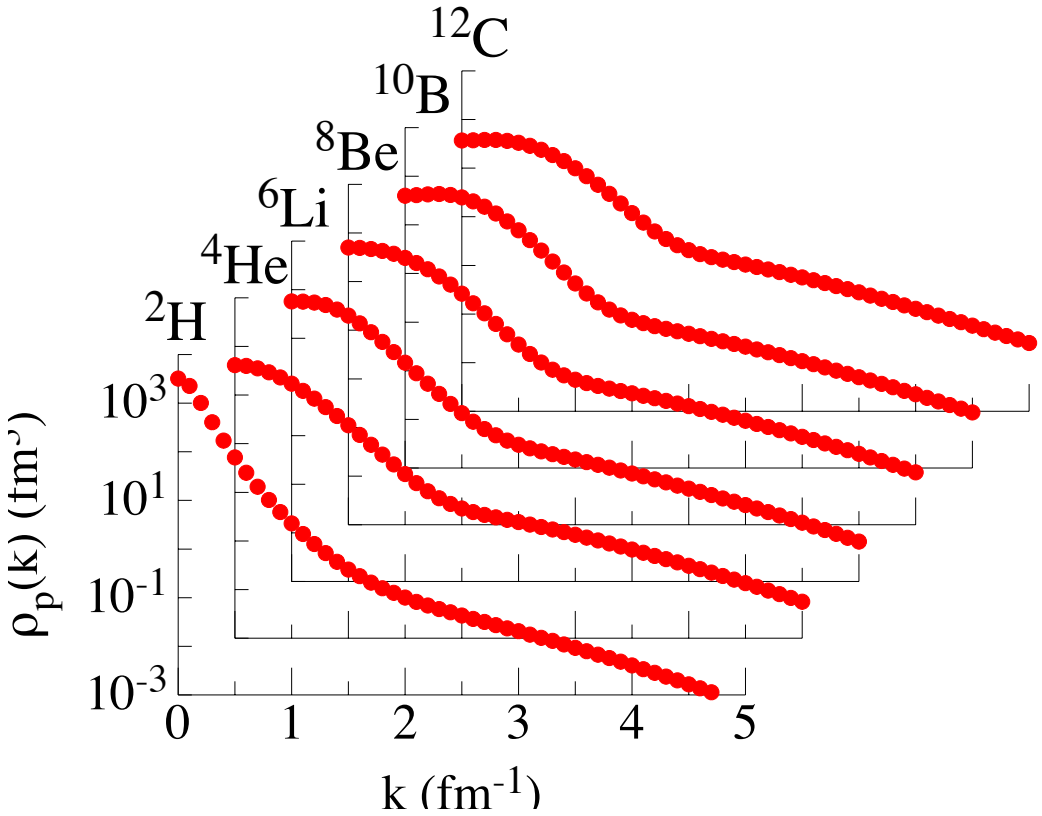

FIG. 3: Nucleon momentum distributions in s- and p-shell nuclei.

correlations associated with the central, spin- and isospin-dependent repulsive components of v_{ij} [14].

The role of the tensor force becomes strikingly apparent when considering the momentum distributions of back-to-back np and pp pairs in nuclei [16] in Fig. 4. The momentum distribution of np pairs is much larger than that of pp pairs for relative momenta in the range of 1.5–3.0 fm^{-1}. The nodal structure present in the pp momentum distribution is absent in the np one, which instead exhibits a change in slope at a characteristic value of $q \simeq 1.5$ fm^{-1}. In nuclei pp pairs are either in spin S=0 and isospin T=1 states or in ST=(11) states: the tensor force vanishes in ST=(01) and is weak in ST=(11), since the two protons must be in relative P-wave (or a higher odd partial wave). On the other hand, most of the np pairs are in deuteron-like states [17] for which the tensor force is strongest, since it can act in relative S-wave. This is best illustrated by a calculation based on a

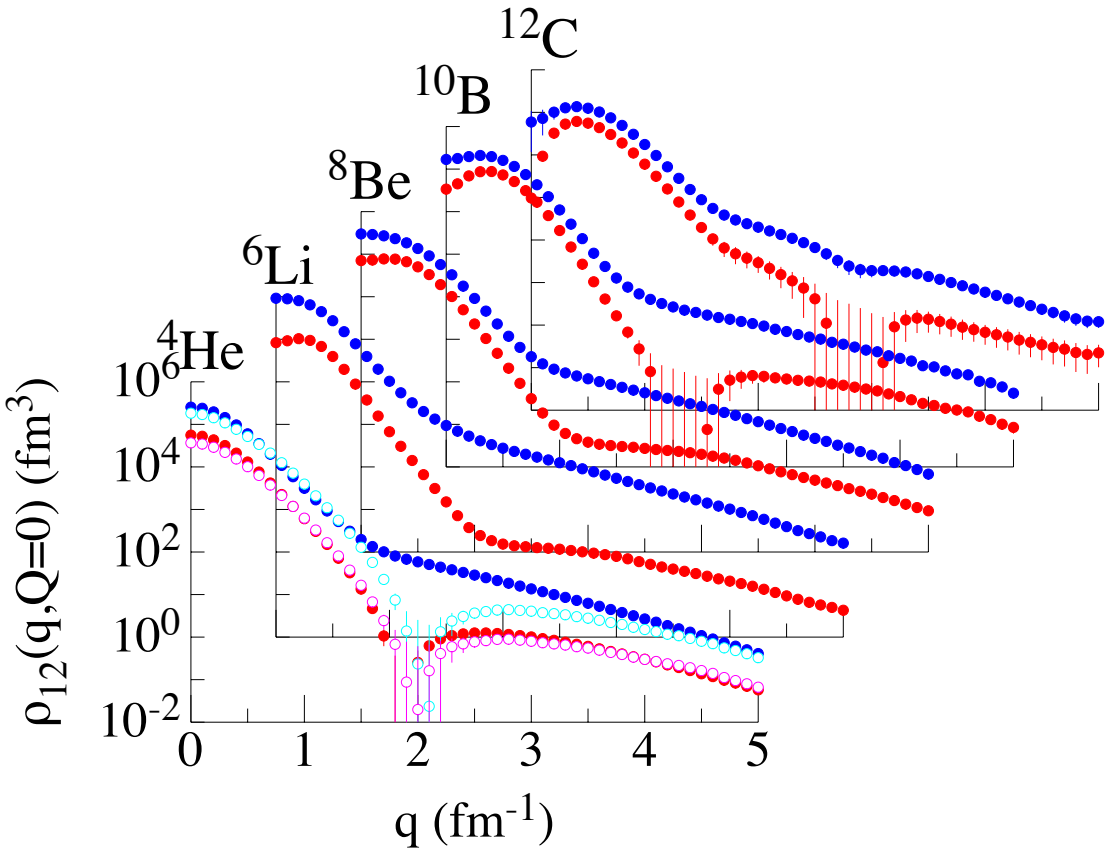

FIG. 4: The momentum distributions of np and pp pairs in s- and p-shell nuclei for vanishing total momentum (back-to-back configuration) and averaged over the directions of the relative momentum $\mathbf{q}$, as function of the magnitude q. Also shown for ^{4}He is the np momentum distribution corresponding to the AV4′ potential with no tensor component.

semi-realistic potential with only central spin- and isospin-dependent terms but no tensor term (it is denoted as AV4′ below). This potential reproduces [18] the empirical S-wave phase shifts and deuteron binding energy but with only an S-state component; the D-state, induced by the tensor force, is absent. While the AV4′ pp momentum distribution, shown for ^{4}He only in Fig. 4, is similar to that obtained with the full AV18 except at the lowest q owing to binding effects, the np momentum distribution develops a node due to the purely S-wave nature of the deuteron-like state [16].

III. PROBING THE SHORT-RANGE STRUCTURE BY NEUTRINOS

Two-nucleon knock-out from high-energy scattering processes is the most appropriate venue to probe nucleon-nucleon (NN) correlations in nuclei. These two-nucleon emissions can occur primarily via two mechanisms that will be reviewed hereafter.

The first type of two-nucleon emission mechanism is one in which the external probe momentum and energy transfers are absorbed by one of two nucleons in a strongly correlated pair, causing the other (spectator) nucleon to recoil and be ejected with high momentum [19]. More specifically, in a naive plane-wave-impulse-approximation (PWIA) picture the cross section for such a process is proportional to the two-nucleon momentum distribution discussed in the previous section, and is therefore affected by correlations induced by the repulsive core and tensor character of the NN force.

Electron scattering experiments have extensively studied these short-range correlations (SRC's). Latest generation experiments have probed them by triple coincidence reactions of the type $A(e, e'\, np$ or $pp)A-2$, in which the two knocked-out nucleons are detected at fixed angles. The SRC pair is typically assumed to be at rest prior to scattering and the kinematical reconstruction utilizes pre-defined four-momentum transfer components determined from the fixed beam energy and the electron scattering angle and energy. The NN SRC's are identified by the detection of a pair of high-momentum nucleons, whose *reconstructed* initial momenta are back-to-back and exceed the characteristic Fermi momentum of the parent nucleus, while the residual nucleus is assumed to be left in a highly excited state after the interaction [22]. Recent results from JLab (on ^{12}C) indicate that $\sim 20\%$ of the nucleons (for $A \geq 12$) act in correlated pairs, and that for high relative momenta ($\sim$ 400–500 MeV/c) $\sim 90\%$ of such pairs are in the form of iso-singlet $(np)_{I=0}$ SRC pairs, while $\sim 5\%$ are in the form of SRC pp pairs and, by isospin symmetry, it is inferred that the remaining $\sim 5\%$ are in the form of SRC nn pairs [23]. These results are consistent with PWIA expectations: the np momentum distribution is an order of magnitude larger than the pp one in back-to-back configurations and relative momenta in the range of the JLab experiment, see Fig. 4.

The second set of two-nucleon emission mechanisms occur via absorption of the external probe momentum and energy transfers by a nucleon pair via a two-body mechanism induced by meson exchange (for example, pion-exchange) or by excitation (de-excitation) of an intermediate nucleon resonance (for example, the Δ resonance), followed (preceded)

by its de-excitation (excitation) via meson emission and the consequent absorption of this meson by a second nucleon [20]. It should be noted that the nucleon-nucleon pairs in these two-body processes may or may not be in a strongly correlated configuration.

The latter mechanism seems to be at play in pion absorption in nuclei, studied extensively over the past several decades in particular at intermediate incident energies (i.e., in the Δ-resonance region). Pion absorption is highly suppressed on a single nucleon, and hence requires at least a two-nucleon interaction. The simplest mechanism (for $A \geq 12$) is on *np* pairs: the so-called quasi-deuteron absorption (QDA), in which, for example, $\pi^+ + (np) \rightarrow pp$. Most of the pion energy is carried away by the ejected nucleons (whose separation energy contributes to the missing energy budget) and part of the momentum can be transferred to the recoil nucleus (missing momentum). Observation from bubble-chamber experiments of pairs of energetic protons with three-momentum $p_{p1}, p_{p2} \gtrsim k_F$ (k_F is the Fermi momentum) detected at large opening angles in the lab frame ($\cos\gamma \lesssim -0.9$) provided first hints for SRC's in the target nucleus [21].

Neutrino scattering experiments only very recently attempted to explore SRC's. The main limitation compared to electron scattering comes from the intrinsic uncertainty on the four-momentum transfer. This originates from the *a priori* undetermined incident neutrino energy. On the other hand, neutrinos (and anti-neutrinos) can effectively probe the nucleus for its SRC content via charge-changing reactions on SRC pairs leading to *two-proton* knock-out topologies. With the advent of LArTPC detectors these signatures can be identified directly and unambiguously. The two protons can indeed be detected *at any emission angle* in the 4π sensitive LAr volume and down to energies below the Fermi level (detection threshold is $T_p^{\rm thr} \simeq 20$ MeV, i.e., well below $k_F \simeq 220$ MeV/c in Ar). This has been first demonstrated by the ArgoNeuT experiment operated in the NuMI beam (3 GeV average neutrino energy) at Fermilab in 2009–2010 and complemented by the magnetized MINOS Near-Detector for muon sign and momentum determination [24, 25].

Using *muon-neutrino* beams, the specific observed reaction is $A(\nu_\mu, \mu^- pp)A-2$ reaction, with the nuclear target $A = {}^{40}$Ar. The final state topology consists of a pair of energetic protons at the interaction vertex accompanying the leading (negative charge) muon. A fraction of the collected events was found compatible with a reconstructed back-to-back configuration of a *np* pair in its *initial state* (CdM frame) inside the nucleus, a signature compatible with one-body quasi-elastic interaction on a neutron in a SRC pair [24], much

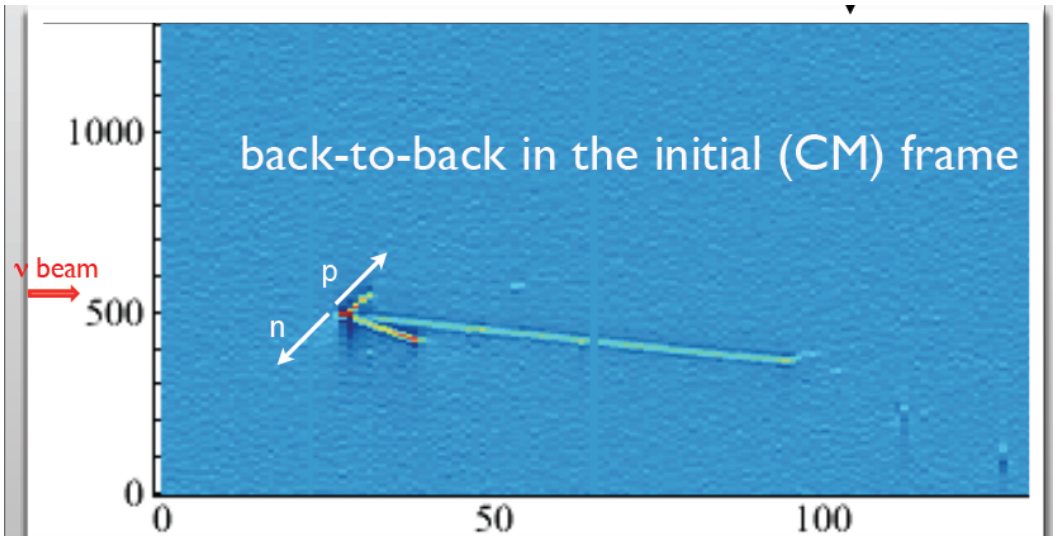

FIG. 5: Two-dimensional views of one of the events with a reconstructed back-to-back np pair in the initial state.

as in the case of the ^{12}C$(e, e' np)$ events observed in the JLab expeirment. This result was indeed obtained with an approach similar to the electron scattering triple coincidence analysis: the initial momentum of the struck neutron was determined by transfer-momentum vector subtraction to the higher proton momentum ($\mathbf{p}_n^i = \mathbf{p}_{p1} - \mathbf{q}$) and the lower momentum proton ($\mathbf{p}_{p2}$) was identified as the recoil spectator nucleon from within SRC, as shown in Fig. 5. The momentum transfer $\mathbf{q}$ is calculated from the reconstructed neutrino energy and the measured muon kinematics.

Another fraction of the $(\mu^- + 2p)$ sample detected with ArgoNeuT were found with the two protons in a strictly back-to-back, high momenta configuration directly observed in the *final state* (lab frame) [24]. Visually the signature of these events gives the appearance of a hammer, with the muon forming the handle and the back-to-back protons forming the head, see Fig. 6 for an example of "hammer" events.

The hammer events are most likely due to pionless (positive charged) resonance mechanisms involving a pre-existing np pair in the nucleus and momentum transfer to the recoil nucleus.

Initial state SRC pairs are nearly at rest, i.e. $\vec{\mathrm{p}}_p^{\,i} \simeq -\vec{\mathrm{p}}_n^{\,i}$. In the case of CC RES processes with no or low momentum transfer to the pair, the events show a large missing momentum and the two protons in final state have momentum significantly above the Fermi momentum, with one almost exactly balanced by the other, i.e. $\vec{\mathrm{p}}_{p1} \simeq -\vec{\mathrm{p}}_{p2}$.
The detection of back-to-back pp pairs in the Lab frame can thus be seen as "snapshots" of

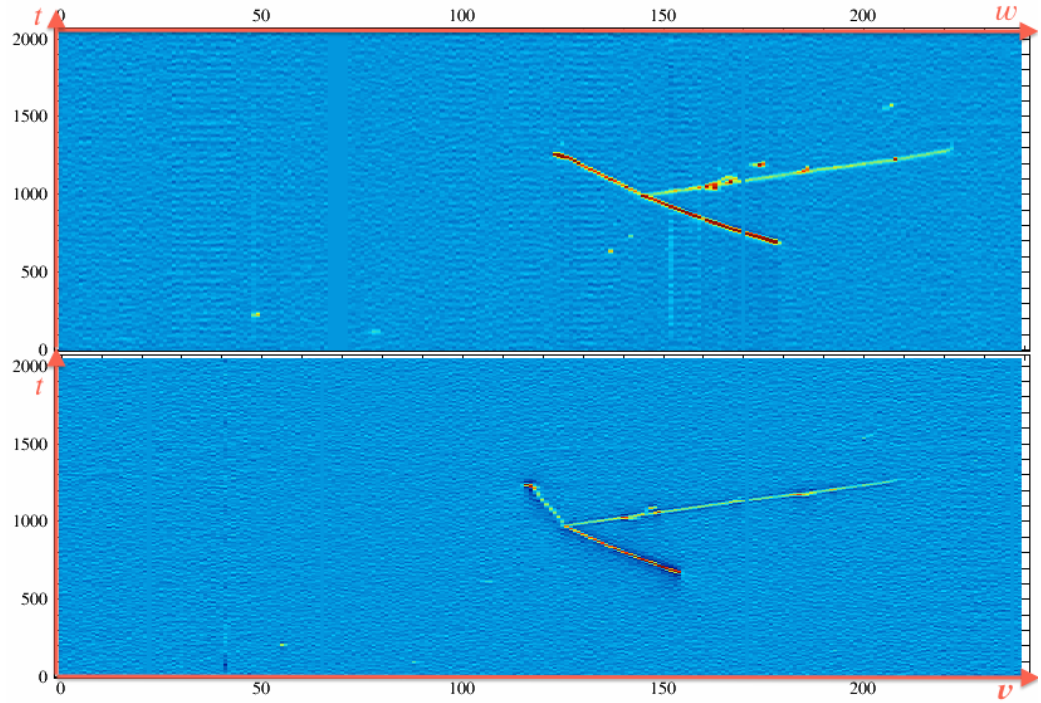

FIG. 6: Two-dimensional views of one of the four "hammer events", with a forward going (negative) muon and a back-to-back proton pair ($p_{p1} = 552$ MeV/c and $p_{p2} = 500$ MeV/c). Transformations from the TPC wire-planes coordinates (*w*,*t* "collection plane" in the top panel; *v*,*t* "induction plane" in the lower panel) into lab coordinates are given in Ref. [25].

the initial *np* pair configuration.

The number of SRC *np* pairs in a nucleus like Ar is large and neutrinos can efficiently detect them. The number of SRC *pp* pairs is much smaller but would be of great interest to directly probe these structures as well.

When switching to a *muon-antineutrino* beam, in general, if the $\overline{\nu}_\mu$ is absorbed by p belonging to a SRC *np*, one should produce two back-to-back neutrons with the same frequency as *pp* with ν_μ. Their detection however may be problematic from an experimental perspective. On the other hand, looking again for back-to-back *two-proton* final state with *muon-antineutrino* beam may be a sensitive signature to *pp* structures.

The charged current reaction of interest is $A(\bar{\nu}_\mu, \mu^+ pp)A-2$, proceeding as through excitation or de-excitation of a nucleon resonance. However, in the anti-neutrino case the formation of a *neutral* resonance (e.g., $W^- p \to \Delta^0$) is required. One can speculate that resonance-excitation processes involving SRC *pp* pairs of the type shown schematically in Fig. 7 could contribute. In these cases two protons would be knocked-out back-to-back, accompanying the leading positive charged muon, with a total of *three positive charge* particles emitted in final state. Indeed, one such event has been found by ArgoNeuT (see Fig.8) with

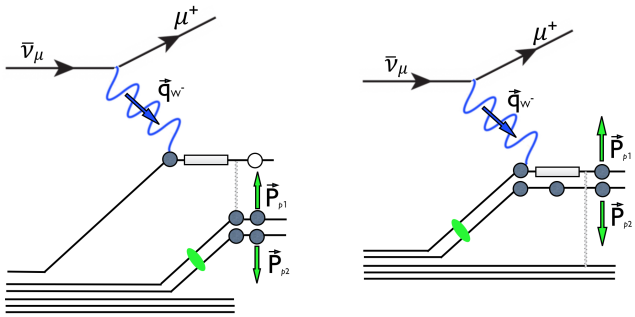

FIG. 7: Pictorial representations of two-proton knock-out charge-changing reactions involving *pp* SRC pairs in antineutrino scattering. Short range correlated nucleon structures in the target nucleus are denoted by the green symbol, full dots for *p*, open dots for *n*, wide solid lines (grey) represent neutral nucleon-resonance states, (gray) lines indicate pions.

the two proton tracks fully contained in the active detector volume and the (positive) charge of the muon unambiguously determined in the downstream MINOS-ND detector.

The detection of these types of events (back-to-back $2p + \mu^-$ and $2p + \mu^+$ shows that mechanisms directly involving SRC pairs (np and pp) in the nucleus are active and can be efficiently explored in neutrino-Ar and antineutrino-Ar interactions with the LAr TPC technology. The event statistics from ArgoNeuT is very limited and cannot provide definitive conclusions. However, larger mass and high statistics LAr-TPC detectors have the opportunity to clarify the issue in the near future. The MicroBooNE experiment with about 70 t of active LAr mass (compared to ArgoNeuT's <0.5 t) is expected to begin operations on the Booster neutrino beam (0.8 GeV average energy) at Fermilab in early 2015. MicroBooNE will be capable of performing a systematic study of SRC (as well as of yet unexplored nuclear effects) at an unprecedented level of detail and statistics. The inclusion of a realistic and exhaustive treatment of SRC in the one- and two-body component of the nuclear current in current theoretical modeling is thus necessary and urgent. The subsequent MC implementation is also extremely important for comparison with liquid argon data.

Improvements in theoretical modeling and MC treatment of these short range phenomena, and comparisons with data, will require sustained collaboration between nuclear theorists and neutrino experimentalists. The extensive history of studying this area of nuclear physics in electron- and hadron-scattering experiments, coupled with the transformative capabilities of LArTPCs to identify neutrinos, will provide collaborators in this endeavor a ripe

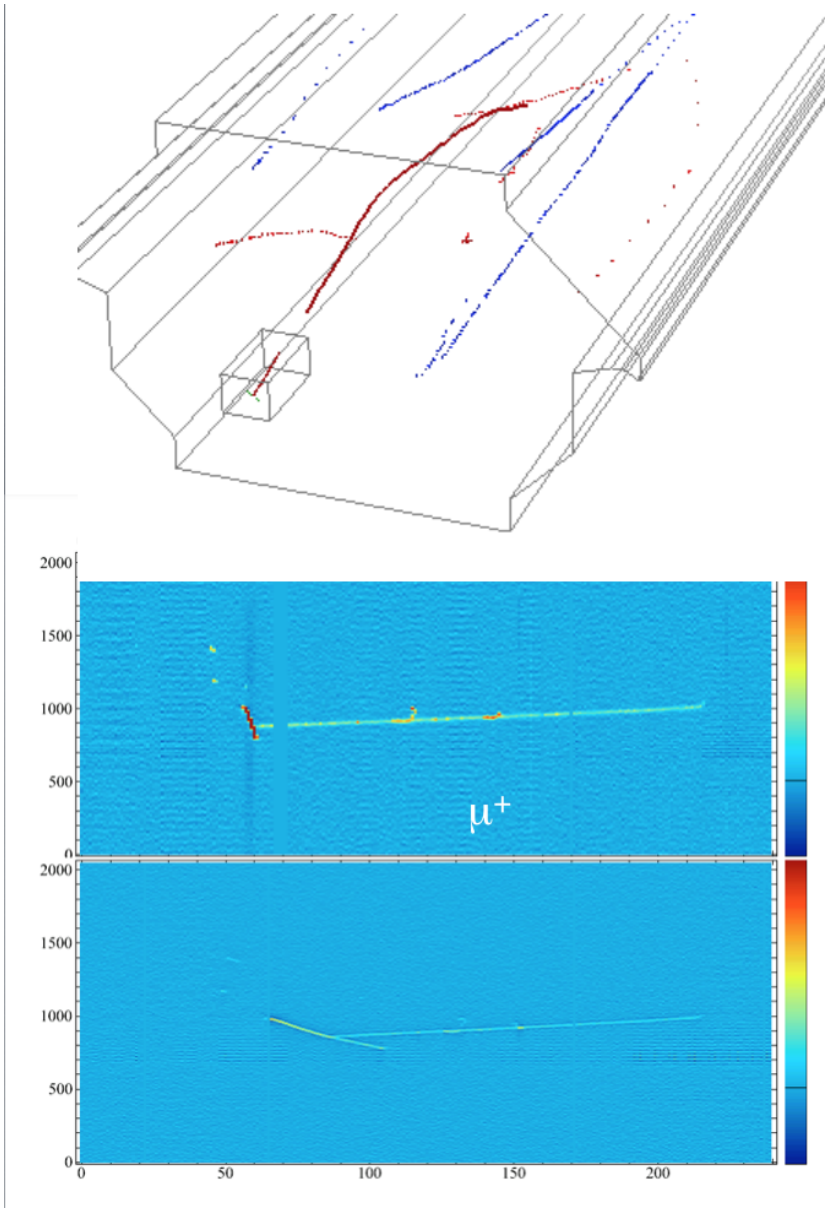

FIG. 8: Three- and two-dimensional views of an antineutrino "hammer event", with a forward going positive muon (positive charged particles in MINOS-ND are recognized by curvature in magnetic field, red tracks for positive sign) and a back-to-back proton pair fully contained in the ArgoNeuT TPC active volume.

opportunity for new discoveries that will further our understanding of the nucleus.

---

[1] E. Rutherford, Phil. Mag. (Series 6) **21**, 669 (1911).

[2] R.B. Wiringa, V.G.J. Stoks, and R. Schiavilla, Phys. Rev. C **51**, 38 (1995).

[3] R. Machleidt, Phys. Rev. C **63**, 024001 (2001).

[4] D.R. Entem and R. Machledt, Phys. Rev. C **68**, 041001 (2003); R. Machleidt and D.R. Entem, Phys. Rep. **503**, 1 (2011).

[5] S.C. Pieper and R.B. Wiringa, Ann. Rev. Nucl. Part. Sci. **51**, 53 (2001).

[6] L.E. Marcucci, A. Kievsky, L. Girlanda, S. Rosati, and M. Viviani, Phys. Rev. C **80**, 034003 (2009).

[7] St. Kystrin *et al.*, Phys. Rev. C **72**, 044006 (2005).

[8] A. Akmal, V.R. Pandharipande, and D.G. Ravenhall, Phys. Rev. C **58**, 1804 (1998).

[9] S.C. Pieper, AIP Conf. Proc. **1011**, 143 (2008).

[10] H. Krebs, A. Gasparyan, and E. Epelbaum, Phys. Rev. C **85**, 054006 (2012).

[11] J. Carlson, et al., arxiv:1412.3081, (submitted to Rev. Mod. Phys.)

[12] A. Lovato, S. Gandolfi, R. Butler, J. Carlson, E. Lusk, S.C. Pieper, and R. Schiavilla, Phys. Rev. Lett. **111**, 092501 (2013).

[13] J.L. Forest, V.R. Pandharipande, S.C. Pieper, R.B. Wiringa, R. Schiavilla, and A. Arriaga Phys. Rev. C **54**, 646 (1996).

[14] R.B. Wiringa, R. Schiavilla, S.C. Pieper, and J. Carlson, Phys. Rev. C **89**, 024305 (2014).

[15] M. Alvioli, C. Ciofi degli Atti, L.P. Kaptari, C.B. Mezzetti, and H. Morita, Phys. Rev. C **87**, 034603 (2013).

[16] R. Schiavilla, R.B. Wiringa, S.C. Pieper, and J. Carlson, Phys. Rev. Lett. **98**, 132501 (2007).

[17] R.B. Wiringa, Phys. Rev. C **73**, 034317 (2006).

[18] R.B. Wiringa and S.C. Pieper, Phys. Rev. Lett. **89**, 182501 (2002).

[19] O. Benhar, A. Lovato, and N. Rocco, arXiv:1312.1210 [nucl-th] (2013).

[20] M. Martini, M. Ericson, G. Chanfray, and J. Marteau, Phys. Rev. C **81**, 045502 (2010).

[21] E. Bellotti *et al.*, Nuovo Cimento **18A**, 75 (1973).

[22] J. Arrington *et al.*, Progr. Part. Nucl. Phys. **67**, 898 (2012).

[23] R. Subedi *et al.*, Science 320, 1476 (2008).

[24] ArgoNeuT Coll. (R. Acciarri *et al.*), Phys. Rev. D 90, 012008 (2014).

[25] ArgoNeuT Coll. (C. Anderson *et al.*), 2012 JINST 7 P10019.